Measuring Rectangularity

Paul L. Rosin
Department of Information Systems and Computing,
Brunel University
UK
email: Paul.Rosin@brunel.ac.uk

Abstract

Three new methods for measuring the rectangularity of regions are developed. They are tested together with the standard minimum bounding rectangle method on synthetic and real data. It is concluded that while all the methods have their drawbacks the best two are the bounding rectangle and discrepancy methods.

1 Introduction

If good and reliable image segmentation is available a popular approach to object classification is based on analysing the shape of the extracted regions (or equivalently the boundaries) [15]. The benefits are

- that the calculation of many of the shape descriptors described in the literature is both simple and efficient, and
- there is a wide choice of techniques for classification based on a vector of properties, and again many are both simple and efficient.

Many shape descriptors have been proposed [1, 14, 20] such as eccentricity, Euler number, compactness, convexity, and bending energy, as well as properties based on moments, Fourier descriptors, circular autoregression, chord distributions, etc. Generally, one of the aims when developing a shape descriptor is to make it invariant to certain transformations or variations. This allows the descriptor to be more generally useful, and reduces the amount of preprocessing otherwise required to normalise the data. For instance, many of the standard shape descriptors listed above are not affected by similarity transformations (scaling, translation, and rotation). However, it is not easy to quantify perceptual shape judgements made by humans, and the research into the representation of shape is ongoing both in the areas of computational vision [11, 23] and biological vision [2, 3, 5, 13, 24].

One approach to shape representation is to define a set of standard shapes such as rectangles or ellipses against which input regions are compared [22]. In the computer vision literature there are standard computational methods for measuring circularity [9], ellipticity [16], and rectangularity [20]. While these work fairly well, care has to be taken in their use. For instance, one of the most popular properties, compactness which is often used to measure circularity, can actually respond better to octagons rather than circles when presented with quantised data [19], and moreover, is sensitive to noise.

While some research has been carried out regarding circularity and ellipticity, rectangularity has been relatively neglected. Many textbooks and surveys do not describe or even mention it as a shape measure [1, 10, 14]. None the less, rectangularity can be a useful property, and can be applied to a range of tasks as diverse as industrial inspection and the discrimination of fish [18].

This paper provides two contributions. First, three new methods for estimating rectangularity of regions are developed. Then together with the standard method all four are evaluated on synthetic and real data to determine how well they behave under noise and various distortions of the shapes.

2 Rectangularity Measures

2.1 Minimum Bounding Rectangle Method (R_B)

The standard method (which we will denote R_B) for estimating rectangularity is to use the ratio of the region's area against the area of the its minimum bounding rectangle (MBR). Although early algorithms

for generating the MBR were quadratic [8] more recently an optimal, linear algorithm has been described by Toussaint [21].

A weakness of using the MBR is that it is very sensitive to protrusions from the region. Even a narrow spike sticking out of a region can vastly inflate the area of the MBR, and thereby produce very poor rectangularity estimates. Moreover, there is an asymmetry between protrusions and indentations, since the latter can have no effect on the MBR (although of course the rectangularity measure is affected).

2.2 Agreement Method (R_A)

Our first new approach assumes that the region is rectangular and measures the lengths of the region's sides in two different ways. If the region really is rectangular then the two sets of measurements should agree. Therefore, rectangularity is defined as the degree of agreement between the estimates $\{a_1, b_1\}$ and $\{a_2, b_2\}$ and is calculated as

$$R = \frac{|a_1 - a_2|}{a_1 + a_2} + \frac{|b_1 - b_2|}{b_1 + b_2}.$$

A value of zero is produced for an exact rectangle while increasing values correspond to less rectangular figures. In order to produce values more easily comparable with the other measures we modify the measure to

$$R_A = 1 - \frac{R}{2}$$

which peaks at one for perfect rectangles.

One way to estimate the sides is to find the image ellipse corresponding to the region. This is an ellipse with the same first and second order moments as the region [17]. From the semi-major and semi minor axes α and β of the ellipse we can then estimate the rectangle's measurements a_1 and b_1 as

$$a_1 = \sqrt{3}\alpha = \sqrt{\frac{6[\mu_{20} + \mu_{02} + \sqrt{(\mu_{20} - \mu_{02})^2 + 4\mu_{11}^2}]}{\mu_{00}}}$$

$$b_1 = \sqrt{3}\beta = \sqrt{\frac{6[\mu_{20} + \mu_{02} - \sqrt{(\mu_{20} - \mu_{02})^2 + 4\mu_{11}^2}]}{\mu_{00}}}.$$

where μ_{pq} are the central moments of the region [17].

Our second estimation method uses the area A and perimeter P of the region. Again, assuming the region is a true rectangle, then since $A = ab$ and $P = 2(a + b)$ we can solve to find a and b in terms of A and P

$$\begin{aligned} a_2 &= \frac{P\sqrt{P^2 - 16A}}{4} \\ b_2 &= \frac{A}{a_2}. \end{aligned}$$

The region's perimeter is calculated using Dorst and Smeulder's method [4]. However, it should be noted that although reliable estimates of area can be made (errors tend to cancel out) it is more difficult to estimate the perimeter as the measurement is sensitive to quantisation and noise effects [6]. For instance, increasing resolution is liable to inflate the perimeter estimate. Similar problems relating to quantisation and noise arose in the measurement of circularity [9, 19].

A second problem with this approach is that it breaks down for shapes more compact than a square. Real, non-zero solutions to the quadratic equation only occur when $\frac{P^2}{16A} > 1$. For instance, for a circle this quantity is $\frac{\pi}{4} \approx 0.7854$.

2.3 Moments Method (R_M)

Our second approach is based on characterising the shape by its moments [17]. The moments of a rectangle centred at the origin and aligned with the axes are $m_{00} = ab$ and $m_{22} = \frac{a^3 b^3}{144}$. This allows us to define a measure of rectangularity

$$R = 144\frac{m_{22}}{m_{00}^3}$$

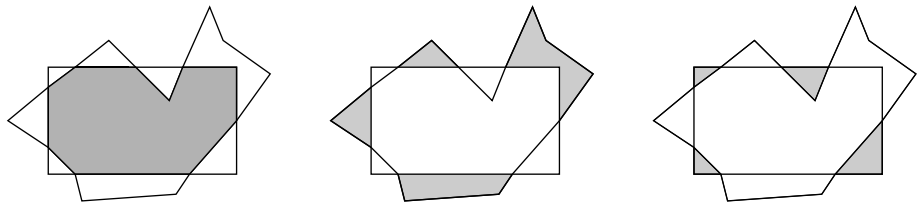

Figure 1: Subregions used to measure discrepancy between region and rectangle

which will return a response of one irrespective of the aspect ratio and scaling of the rectangle. To make the descriptor invariant to rotation and translation we must first normalise the data. This can easily be done using moments to calculate the centroid $(\bar{x}, \bar{y})$ and orientation θ of the data as

$$\begin{aligned} \bar{x} &= \frac{m_{10}}{m_{00}} \\ \bar{y} &= \frac{m_{01}}{m_{00}} \\ \theta &= \frac{1}{2}\tan^{-1}\frac{2\mu_{11}}{2\mu_{20} - 2\mu_{02}} \end{aligned}$$

so that the data can then be translated by $(-\bar{x}, -\bar{y})$ and rotated by $-\theta$. Again, to make the measure more convenient to interpret we apply the following transformation that ensures that the descriptor peaks at one for true rectangles while non-rectangles return values in the range $(0, 1)$

$$R_M = \begin{cases} R & \text{if } R \leq 1 \\ \frac{1}{R} & \text{otherwise} \end{cases} .$$

2.4 Discrepancy Method (R_D)

Our third approach has a similar motivation to the bounding rectangle method. A rectangle is fitted to the region, and the discrepancies between the rectangle and region are measured. In an attempt to overcome the weaknesses of the bounding box as a region description, instead we fit the rectangle using the image ellipse described above. The lengths of the sides are as given in section 2.2, and the centre and orientation are also calculated using moments as shown in section 2.3. Whereas the bounding rectangle circumbscribes the region the image ellipse rectangle will pass through the region, hopefully providing a more representative fit.

The fitted rectangle is used to clip the region. Standard algorithms are available for clipping and polygon intersection [7, 12]. The following areas are then measured: A_1 - the complete region, A_2 - the clipped region, and A_3 - the rectangle.[1]

The discrepancy between the region and the fitted rectangle consists of two parts: the area of the region outside the rectangle $A_1 - A_2$, and the area of the rectangle that is not filled by the region $A_3 - A_2$. We normalise the errors by the size of the rectangle, and subtract from one so as to peak at one, to get

$$R_D = 1 - \frac{A_1 + A_3 - 2A_2}{A_3}.$$

3 Evaluation

We evaluate the measures by applying them to some parameterised synthetic shapes. This enables us to track the rectangularity values as we continuously modify the shapes. We start with a superellipse, defined by the implicit equation

$$\left(\frac{x}{a}\right)^{\frac{2}{\epsilon}} + \left(\frac{y}{b}\right)^{\frac{2}{\epsilon}} = 1.$$

[1] We have simplified our implementation by calculating approximations to these quantities by performing image based operations rather than directly manipulating the boundaries.

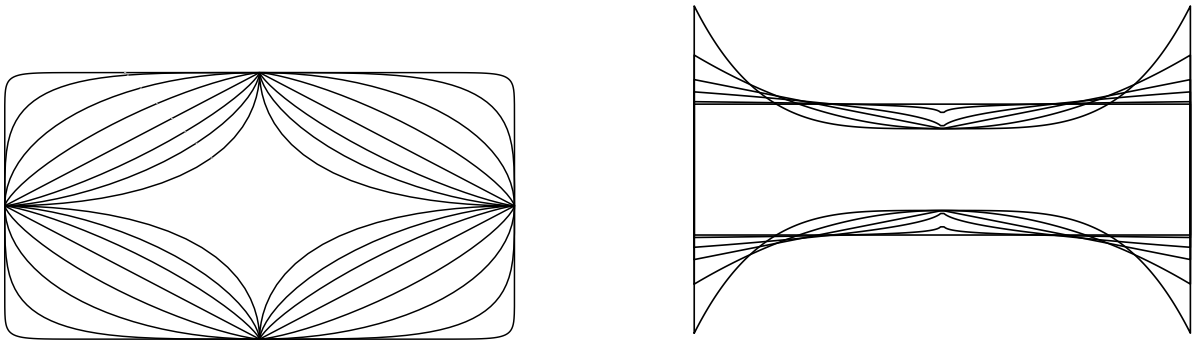

(a) Superellipse shapes

(b) Polynomial pair shapes

Figure 2: The continuum of shapes generated to show deformations from a rectangle

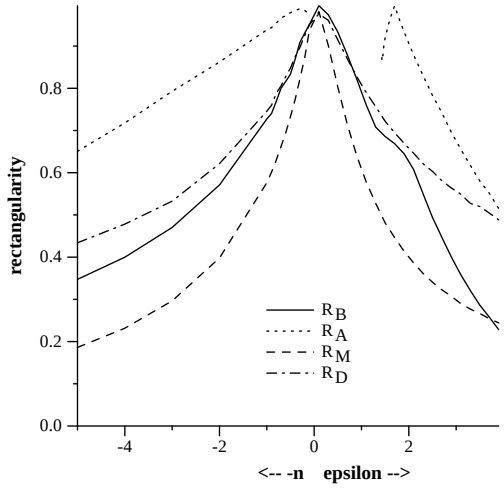

Figure 3: Measured rectangularity of synthetic shapes over a range of deformations from a rectangle

A value of $\epsilon = 0$ produces a true rectangle. Increasing ϵ corresponds to lopping off the corners, which can also be viewed as squeezing increasing amounts of the region towards the centre (and rescaling, which we can ignore).

The second shape has been defined to vary in the opposite manner. We use a polynomial

$$y = cx^n + d$$

which is also duplicated and reflected in the X-axis, and the two are connected to form a region. Increasing n corresponds to squeezing increasing amounts of the region outwards from the centre. We arbitrarily set $d = \frac{b}{2}$ and the remaining coefficient is set to $c = (\frac{2}{a})^n(1+n)(2bf - d)$ so as to fix the region's area to a constant fraction f of the area of the bounding rectangle. Examples of the region boundaries over a range of the relevant shape parameters are shown in figure 2 for the two sets of shapes.

The graph in figure 3 displays rectangularity against the deformations of the synthetic rectangles. Since both sets of test curves start from the same rectangle we have plotted rectangularity for both sets on the same graph. Right of the origin (increasing ϵ) corresponds to results from shapes like those in figure 2a while left of the origin (increasing $-n$) corresponds to results from shapes like those in figure 2b. Whereas R_B, R_M and R_D operate in a reasonable manner R_A breaks down due to an underestimate of the perimeter which causes the estimation of the rectangle's axis lengths to return an imaginary solution.

We next examine the effect of another deformation of the basic rectangle. The Y coordinate value of one corner is scaled to shift it up and down to create a trapezoid. In contrast to the previous shapes this one is not symmetric (see figure 4a). Both R_B and R_D are again well behaved, peaking at one for a rectangle (see figure 5a). R_M shows little variation in value, only a slight drop-off for extreme values of deformation. Likewise, R_A produces similar rectangularity estimates over the range of trapezoids. But worse than R_M, R_A is extremely sensitive to errors in the perimeter estimation, which (due to the image

(a) trapezoid (b) rectangle with protrusion

Figure 4: Further continuous deformations of the rectangle

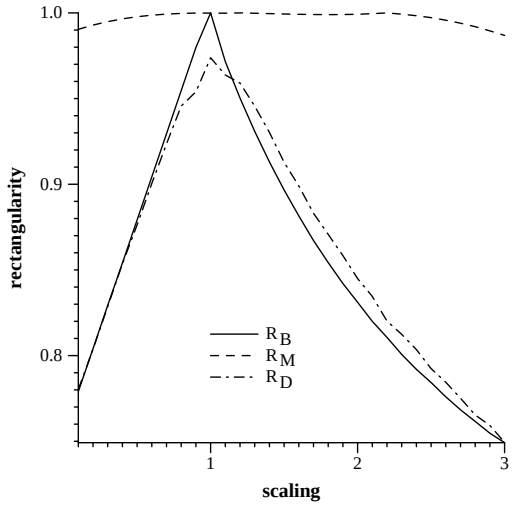

(a) R_B and R_M

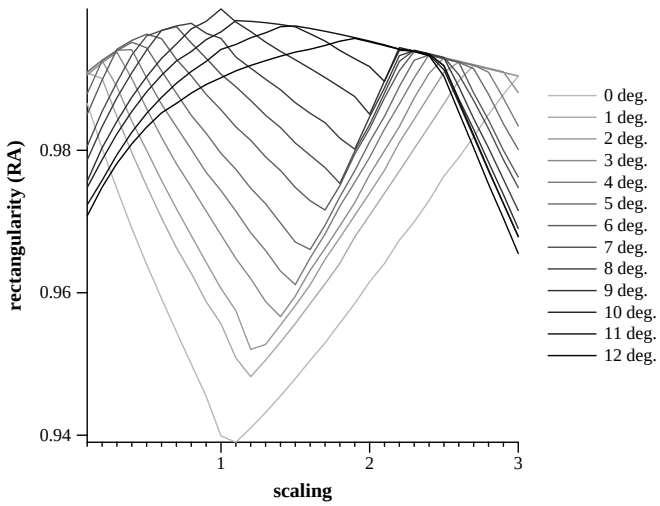

(a) R_A

Figure 5: Rectangularity of trapezoid

quantisation) is a function of the orientation of the region. As figure 5b shows, depending on the rotation of the shape, the measure can as easily be minimised as maximised by an undeformed rectangle.

When the measures are applied to the rectangle with protrusions (figure 4b) the expected asymmetry of the bounding box method is evident (figure 6). Intrusions (indicated by negative values of protrusion) have little effect on the rectangularity measurement but protrusions have a large effect. The moments and discrepancy methods are also affected in a similar way, but to a much smaller degree. Although the agreement method appears symmetric it shows a dip for a real rectangle. This occurs because the perimeter was underestimated at that point. The peak value occurs when the inaccurate perimeter estimate matches the expected value for the undeformed rectangle.

We examine the effects of noise by testing the methods on a rectangle and ellipse with varying degrees of added noise. The two extremes of noise are illustrated in figure 7. The agreement method does poorly, as it is unable to reliably discriminate between the rectangle and ellipse. Although the other three methods do consistently discriminate the two shapes it can be seen that the difference in R_B values becomes small as the level of noise increases. In contrast, the R_M and R_D values are not substantially affected by noise.

The above experiments have all been performed on synthetic data. The final test is to apply the measures to 56 regions extracted from a variety of images, and displaying a range of shapes, and noise levels. Figure 9 shows the regions ranked into descending order according to the rectangularity measures. Based on a qualitative judgement the bounding rectangle and discrepancy methods appear best, followed by the agreement method, while the moment based method fares worst.

4 Conclusions

Three new rectangularity measures have been developed, and together with the standard method, all four have been evaluated on both synthetic and real data. From the real data the bounding rectangle and

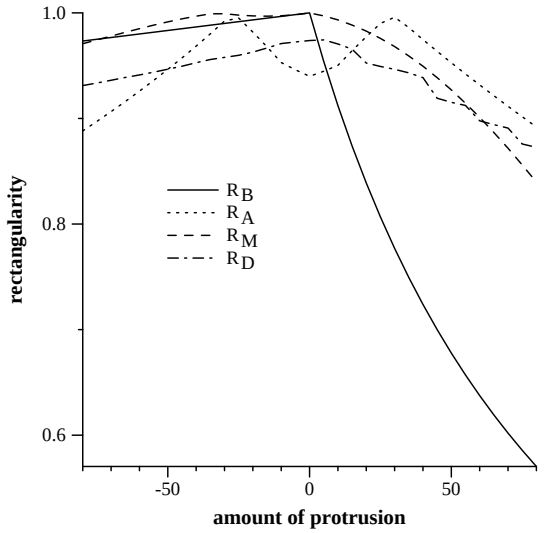

Figure 6: Measured rectangularity of rectangles containing a range of indentations/protrusions

Figure 7: Samples of noisy rectangles and ellipses

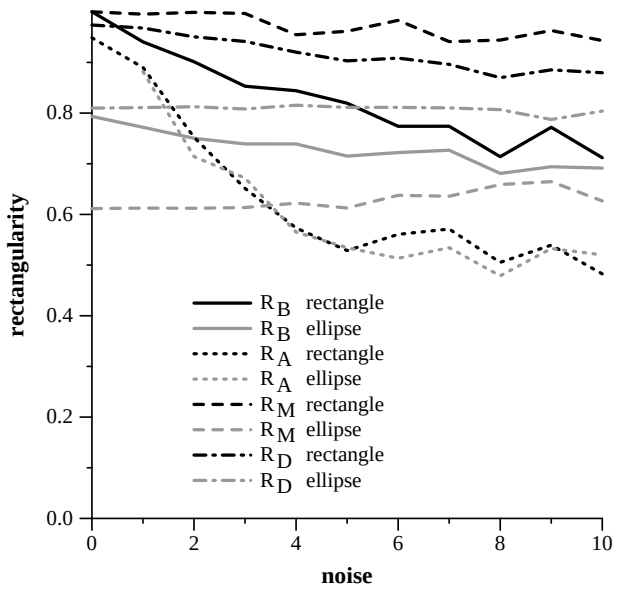

Figure 8: Measured rectangularity of noisy rectangles and ellipses

discrepancy methods rate best. However, the tests on synthetic data confirm or reveal that each method has several shortcomings:

- The bounding box method responds unequally to protrusions and indentations, and is sensitive to noise – especially protrusions.
- The agreement method breaks down for compact regions, and is prone to errors due to inaccuracies in the perimeter estimation. The errors are a function of both the region's orientation and resolution.
- The moment based method can respond to other shapes as well as rectangles if they have a similar ratio of moments. For compact shapes (e.g. the near square on the bottom row) the orientation estimation is sensitive to noise, which can lead to incorrect rectangularity estimates.
- The discrepancy method uses moments to estimate the rectangle fit, and is similarly prone to poor orientation estimates for compact shapes.

Since the errors incurred by the orientation estimator for compact shapes tend to be around 45° a simple correction can be applied. An incorrect orientation estimate lowers the rectangularity measure. Therefore the rectangularity of a region can be measured both at its estimated orientation and also after an additional 45° rotation. Only the maximum rectangularity is retained. This modification was applied to the methods R_M and R_D, and their results are shown in figure 9 labelled as R'_M and R'_D. A significant improvement is seen – many compact shapes are now correctly ranked. However, the general conclusions from section 3 remain the same: the methods of choice are either R_B or R'_D.

References

[1] D.H. Ballard and C.M. Brown. *Computer Vision*. Prentice Hall, 1982.

[2] J.M. Cortese and B.P. Dyre. Perceptual similarity of shapes generated from Fourier descriptors. *Journal of Experimental Psychology*, 22(1):133–143, 1996.

[3] J.E. Cutting and J.J. Garvin. Fractal curves and complexity. *Perception & Psychophysics*, 42(4):365–370, 1987.

[4] L. Dorst and A.W.M. Smeulders. Length estimators for digitized contours. *Computer Vision, Graphics and Image Processing*, 40(3):311–333, 1987.

[5] G. Dudek, M. Arguin, and D. Bub. Human integration of shape primitives. In C. Arcelli *et al.*, editor, *Aspects of Visual Form Processing*, pages 188–198. World Scientific, 1994.

[6] T.J. Ellis, D. Proffitt, D. Rosen, and W. Rutkowski. Measurement of the lengths of digitized curved lines. *Computer Graphics and Image Processing*, 10:333–347, 1979.

[7] J.D. Foley and A. van Dam. *Fundamentals of Interactive Computer Graphics*. Addison-Wesley, 1982.

[8] H. Freeman and R. Shapira. Determining the minimum-area encasing rectangle for an arbitrary curve. *Comm. ACM*, 18:409–413, 1975.

[9] R.M. Haralick. A measure for circularity of digital figures. *IEEE Transactions on Systems, Man and Cybernetics*, 4:394–396, 1974.

[10] R.M. Haralick and L.G. Shapiro. *Computer and Robot Vision*. Addison Wesley, 1992.

[11] B.B. Kimia, A.R. Tannenbaum, and S.W. Zucker. Shapes, shocks, and deformations. *International Journal of Computer Vision*, 15(3):189–224, 1995.

[12] M.V. Leonov and A.G. Nikitin. An efficient algorithm for a closed set of boolean operations on polygonal regions in the plane. Technical Report Preprint 46, Novosibirsk, A. P. Ershov Institute of Informatics Systems, 1997.

[13] N.A. MacMillan and D.S. Ornstein. The mean-integral representation of rectangles. *Perception & Psychophysics*, 60(2):250–262, 1998.

[14] S. Marshall. Review of shape coding techniques. *Image and Vision Computing*, 7(4):281–294., 1989.

[15] M. Peura and J. Iivarinen. Efficiency of simple shape descriptors. In C. Arcelli *et al.*, editor, *Aspects of Visual Form Processing*. World Scientific, 1997.

[16] D. Proffitt. The measurement of circularity and ellipticity on a digital grid. *Pattern Recognition*, 15(5):383–387, 1982.

[17] R.J. Prokop and A.P. Reeves. A survey of moment-based techniques for unoccluded object representation and recognition. *CVGIP: Graphical Models and Image Processing*, 54(5):438–460, 1992.

[18] R.A. Richards and C. Esteves. Use of scale morphology for discriminating wild stocks of atlantic striped bass. *Trans. Amer. Fisheries Soc.*, 127(6):919–925, 1997.

[19] A. Rosenfeld. Compact figures in digital pictures. *IEEE Transactions on Systems, Man and Cybernetics*, 4:221–223, 1974.

[20] M. Sonka, V. Hlavac, and R. Boyle. *Image Processing, Analysis, and Machine Vision*. Chapman and Hall, 1993.

[21] G.T. Toussaint. Solving geometric problems with the rotating calipers. In *Proc. IEEE MELECON '83*, pages A10.02/1–4, 1983.

[22] E.E. Underwood. *Quantitative Stereology*. Addison-Wesley, 1970.

[23] A. Verri and C. Uras. Metric-topological approach to shape representation and recognition. *Image and Vision Computing*, 14(3):189–207, 1996.

[24] D.J. Weintraub. Rectangle discriminability: perceptual relativity and the laws of Prägnanz. *J. Experimental Psychology*, 88:1–11, 1971.

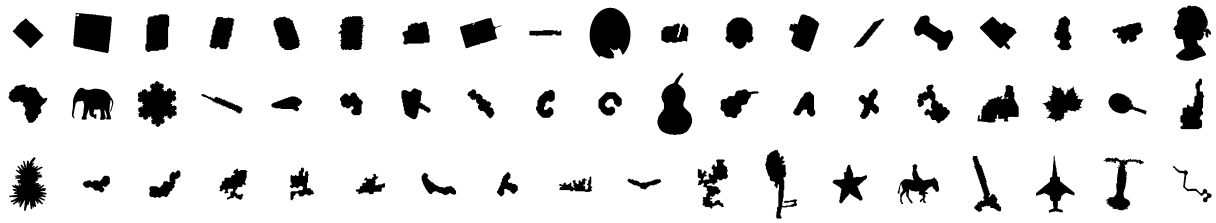

R_B

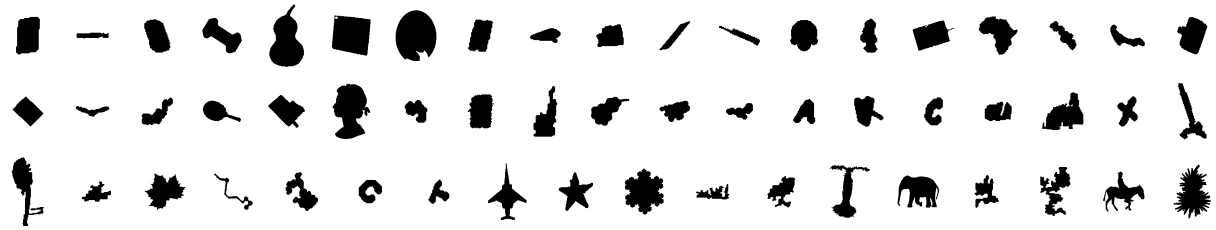

R_A

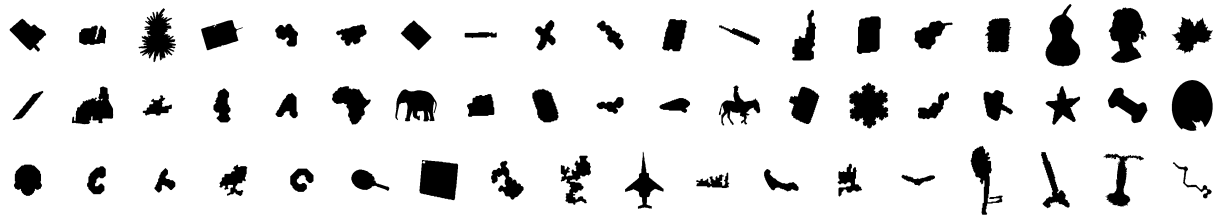

R_M

R'_M

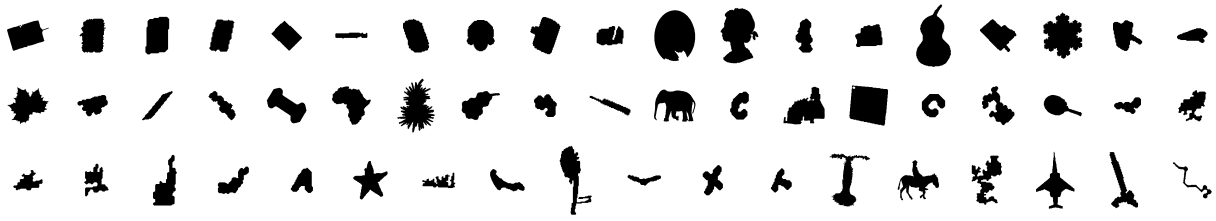

R_D

R'_D

Figure 9: Ranking of shapes according to various rectangularity measures